Shorter Exciton Lifetimes via an External Heavy-Atom Effect: Alleviating the Effects of Bimolecular Processes in Organic Light-Emitting Diodes

Citation: Einzinger, Markus et al. "Shorter Exciton Lifetimes via an External Heavy-Atom Effect: Alleviating the Effects of Bimolecular Processes in Organic Light-Emitting Diodes." Advanced Materials 29, 40 (September 2017): 1701987 © 2017 WILEY#VCH Verlag

As Published: https://doi.org/10.1002/adma.201701987

Publisher: Wiley Blackwell

Persistent URL: http://hdl.handle.net/1721.1/115110

Version: Author's final manuscript: final author's manuscript post peer review, without publisher's formatting or copy editing

DOI: 10.1002/((please add manuscript number))
Article type: Communication

Shorter Exciton Lifetime via an External Heavy Atom Effect: Alleviating the Effects of Bimolecular Processes in Organic Light Emitting Diodes

Markus Einzinger, Tianyu Zhu, Piotr de Silva, Christian Belger, Timothy M. Swager, Troy Van Voorhis, Marc A. Baldo*

Markus Einzinger, Prof. Dr. Marc A. Baldo
Department of Electrical Engineering and Computer Science
77 Massachusetts Avenue, Massachusetts Institute of Technology
Cambridge, MA 02139, USA.
E-mail: meinzing@mit.edu

Tianyu Zhu, Dr. Piotr de Silva, Dr. Christian Belger, Prof. Dr. Timothy M. Swager, Prof. Dr. Troy Van Voorhis
Department of Chemistry
77 Massachusetts Avenue, Massachusetts Institute of Technology
Cambridge, MA 02139, USA.

Keywords: External Heavy Atom Effect, Spin-Orbit Coupling, Intersystem Crossing, Thermally Activated Delayed Fluorescence, Organic Light Emitting Diodes

Multi-excited state phenomena are believed to be the root cause of two exigent challenges in organic light emitting diodes, namely efficiency roll-off and degradation. The development of novel strategies to reduce exciton densities under heavy load is therefore highly desirable. In this article it is shown that triplet exciton lifetimes of thermally activated delayed fluorescence emitter molecules can be manipulated in solid state by exploiting intermolecular interactions. The external heavy atom effect of brominated host molecules leads to increased spin orbit coupling, which in turn enhances intersystem crossing rates in the guest molecule. Wave function overlap between the host and the guest is confirmed by combined molecular dynamics and density functional theory calculations. Shorter triplet exciton lifetimes are observed, while high photoluminescence quantum yields and essentially unaltered emission spectra are maintained. This leads to almost 50% lower triplet exciton densities in the emissive layer in steady state and results in an improved onset of the PLQY roll-off at

high excitation densities. Efficient organic light emitting diodes with better roll-off behavior based on these novel hosts are fabricated, demonstrating the suitability of this concept for real-world applications.

Excitons are created from the condensation of complementary charge carriers and relax to give the photons emitted from organic light emitting diodes (OLEDs). Since the ground state of almost all organic molecules is of spin quantum number zero, the interconversion of singlet excitons and photons is quantum mechanically allowed. However, considerable populations of long-lived "dark" triplet excitons also play a very important role in organic devices. In OLEDs, roughly 3 out of 4 generated excitons have triplet character as a result of spin statistics.[1] The ability to harness triplet excitons for light generation was first introduced in the form of phosphorescent emitter molecules and led to internal quantum efficiencies (IQEs) of nearly 100%.[2–6] More recently, emitters based on thermally activated delayed fluorescence (TADF) with comparable IQE values have emerged.[7,8] Here, the singlet can be repopulated from the triplet state thermally, as a result of very small singlet-triplet splitting (Figure 1a). The small splitting is achieved by spatially separating the highest occupied molecular orbital (HOMO) and lowest unoccupied molecular orbital (LUMO), which diminishes exchange interaction.[9] The exact mechanism of the reverse intersystem crossing pathway is currently subject to debate. The direct intersystem crossing between the charge transfer states ^{1}CT and ^{3}CT is assumed to be very inefficient due to the vanishing spin-orbit coupling between these states (Figure 1b).[10,11] Efficient reverse intersystem crossing could be explained by hyperfine interactions.[12,13] Moreover, a mediated spin-orbit coupling process involving a higher (or lower) lying local exciton ^{3}LE has emerged as alternative explanation.[14,15]

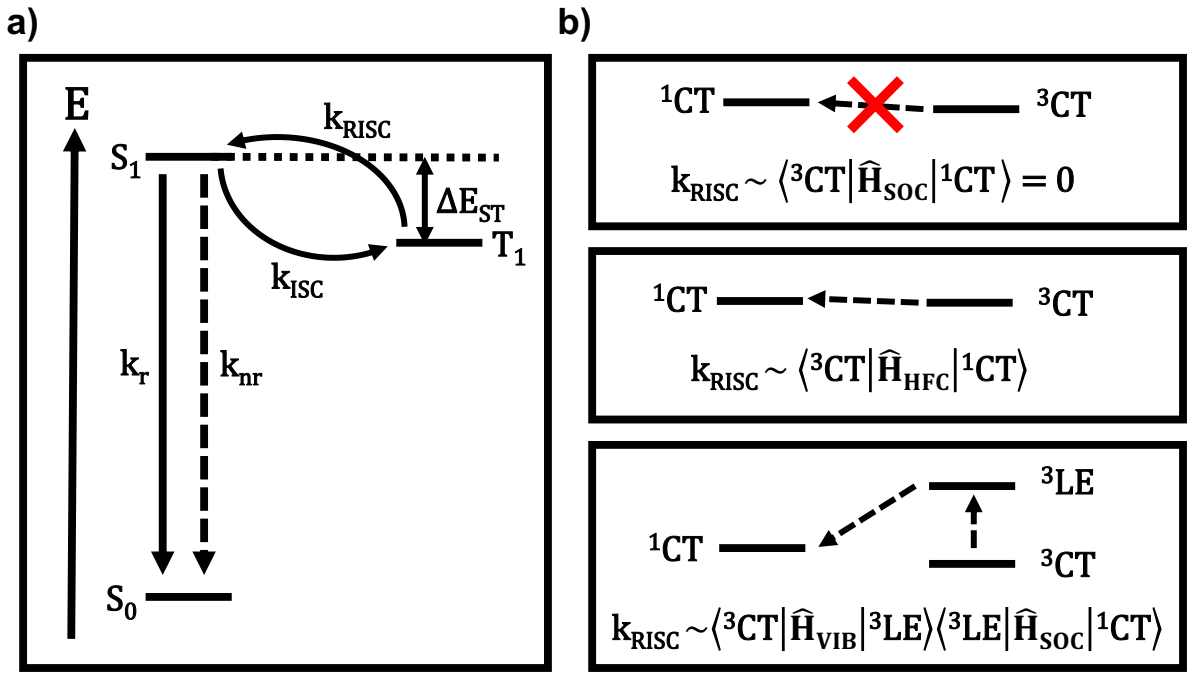

Figure 1. (a) Rate model for TADF process. S_0 is the ground state, S_1 is the singlet energy level, T_1 is the triplet energy level, k_R is the radiative rate, k_{NR} is the non-radiative rate, k_{ISC} and k_{RISC} are the intersystem crossing rate and reverse intersystem crossing rate. **(b)** Three discussed mechanisms for coupling singlet and triplet manifolds. Top: Spin-Orbit Coupling (SOC) between singlet charge transfer state ^{1}CT and triplet charge transfer state ^{3}CT (forbidden). Center: Hyperfine Coupling (HFC). Bottom: Coupling mediated by a locally excited triplet state ^{3}LE.

The triplet exciton lifetimes of both phosphors and TADF emitters are on the order of several microseconds. This is in contrast to the very short exciton lifetimes in fluorescent emitters of only few nanoseconds. As a result of this fairly long triplet exciton lifetime, the exciton density is large. This favors the occurrence of bimolecular events, like triplet-triplet annihilation (TTA) and triplet-charge annihilation (TCA).[16–19] These events are usually undesired and constitute loss processes. One consequence is the well-documented decrease in efficiency under high current densities, often referred to as “droop” or “roll-off”.[20] Moreover, bimolecular processes generate “hot” excitons that are suspected to cause degradation events.[21] It has already been demonstrated that photobleaching can be suppressed by three orders of magnitude by enhancing the spontaneous emission rate.[22]

It is therefore paramount to invent new ways of decreasing exciton lifetimes. This has to be achieved while leaving other properties, like photoluminescence quantum yields (PLQYs), luminescence spectra and electrical behavior unaltered. Further reducing singlet-triplet splitting by reducing HOMO-LUMO overlap could reduce exciton lifetimes by speeding up reverse intersystem crossing, but this strategy usually has the unwanted side effect of reducing the oscillator strength.[23] Notably, it has been shown that intersystem crossing can be enhanced by covalently attaching heavy atoms to emitter molecules.[24] Moreover, it has been well documented that absorption features and photoluminescence behavior of solutions can be influenced by the mere proximity of heavy atoms that are not even covalently bound to the respective molecule.[25–31] This phenomenon is known as the external heavy atom effect. It was already successfully utilized in white OLEDs by combining blue TADF fluorophores and yellow phosphors.[32] However this approach is not applicable to monochrome pixels, as needed in active matrix display applications. An increase in OLED external quantum efficiency (EQE) after the insertion of a heavy atom perturber layer has also been reported.[33] Unfortunately, this approach requires an additional evaporation step and might hamper ideal charge balance factors in devices. We therefore propose to introduce heavy atoms by substituting hydrogen atoms in established host molecules, thereby utilizing the beneficial influence of the heavy atom effect while keeping potential adverse consequences at a minimum level.

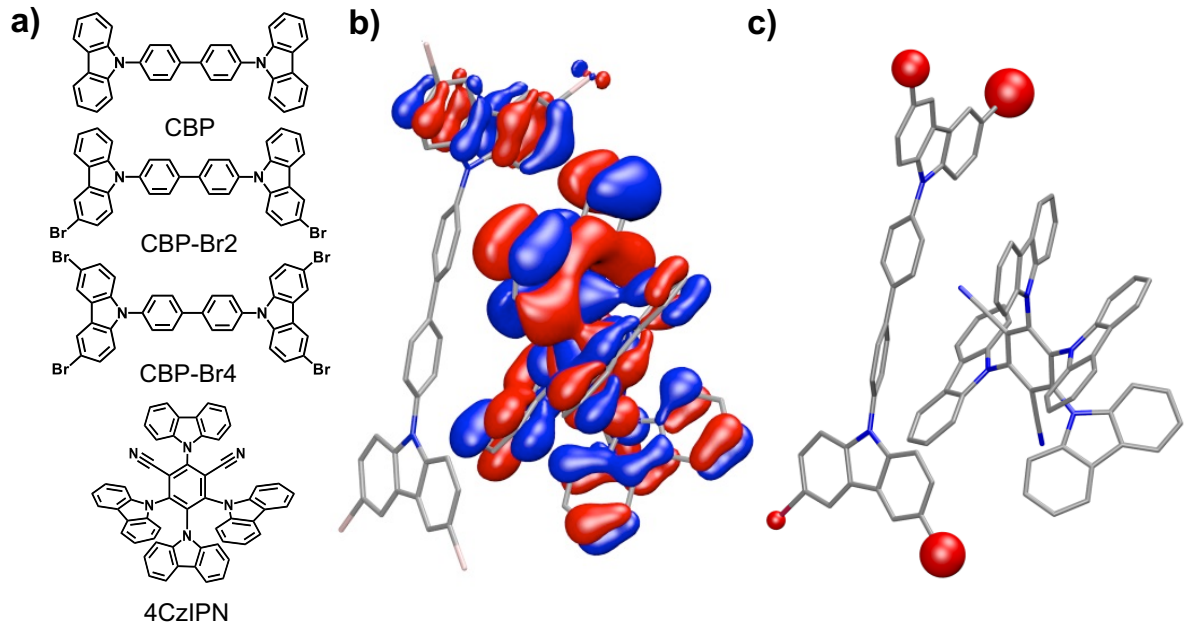

Figure 2. (a) Molecular structures of host and emitter materials employed in this study. **(b)** Orbital (third highest occupied molecular orbital, HOMO-2) delocalizes over both host and guest molecules. Specifically, one Br atom (upper right) is involved in this orbital delocalization. **(c)** The Löwdin charge changes (T_1 state vs. S_0 state) on Br atoms, as shown by red spheres around Br atoms.

We choose the well-known host CBP and its brominated derivatives CBP-Br2 and CBP-Br4 (shown in Figure 2a) to test our hypothesis. These molecules have been used as intermediates in organic syntheses.[34–41] They feature a Br (Z_N=35) content by weight of 0%, 25% and 40% respectively. We measured the first excited triplet state energy levels of CBP, CBP-Br2 and CBP-Br4 by room temperature triplet state spectroscopy.[42] They are determined to be identical at T_1 = 2.55 eV (Figure S13). In case of CBP, this is in excellent agreement with literature (2.58 eV, 2.56 eV).[42,43] Thus, the brominated host molecules have appropriate triplet energy levels to be used as host materials in OLEDs. We also measured the refractive indices of the three host materials by ellipsometry (Figure S15). For any given wavelength, the refractive index is increasing with increasing Br content. The molecule 4CzIPN is an excellent testing emitter, since it features high PLQY and it facilitates high efficiency OLEDs.[7]

In order to confirm that adding Br atoms to the host molecules can in principle affect the spin-orbit coupling in the guest molecule, we employ a combined molecular dynamics (MD) and density functional theory (DFT) computational approach. The heavy atom effect brought by Br atoms in the host can have an influence on the guest only if the excited state wave functions of the guest delocalize over the host. Therefore, we investigate the charge delocalization of the first excited triplet state (T_1) of the 4CzIPN/host (host=CBP, CBP-Br2, CBP-Br4) dimer systems. Our combined MD and DFT calculations show that there are some occupied orbitals of the T_1 state delocalizing over both guest and host molecules (Figure 2b). In particular, specific Br atoms are involved in the orbital delocalization. This result indicates that the states of the guest and brominated host molecules are coupled in the emissive layer (EML). We also performed a Löwdin population analysis of the T_1 state.[44] The Löwdin charge on the host in the 4CzIPN/host dimer systems (averaged over 10 dimer structures for each host) changes from -0.001 *e* to -0.018 *e* when adding two Br atoms to CBP, and it further decreases to -0.025 *e* for CBP-Br4 (Table S1). This decrease is attributed to the strong electronegativity of Br atoms. More importantly, it shows that there is clearly a small amount of charge transfer from 4CzIPN to CBP-Br2 and CBP-Br4 when 4CzIPN is in the T_1 state, indicating that the brominated hosts can have an effect on the spin-orbit coupling in the guest.

Furthermore, we also investigate quantitatively if there is any charge delocalization specifically on Br atoms. We compare the Löwdin charge on Br atoms in the T_1 state of a 4CzIPN/host dimer with that in the S_0 state of the same dimer. The difference of Löwdin charges on Br atoms is therefore considered to reflect the additional charge delocalization when 4CzIPN is in the T_1 state (Table S1). There is a significant amount of relative Löwdin charge difference on Br atoms in both CBP-Br2 (-0.004 *e*) and CBP-Br4 (-0.007 *e*) (Figure 2c), which is evidence that the T_1 state of 4CzIPN specifically delocalizes over Br atoms in

the host. Together, these computational results reveal that the added Br atoms in the host can interact with the guest excited states and contribute to its increased spin-orbit coupling.

In order to experimentally test the influence of the host materials on the emitter molecules, we fabricated doped films with a thickness of 100 nm by thermal evaporation (20wt%). The films show slightly differing absorption features (Figure 3). CBP:4CzIPN exhibits a pronounced peak at 297 nm. This peak is slightly red-shifted in CBP-Br2:4CzIPN and CBP-Br4:4CzIPN to 303 nm and 308 nm respectively. Utilizing the brominated host materials does not appreciably influence the emission spectra, although there is a slight blue-shift with increasing Br content. The emission peak wavelengths are measured to be at 534 nm, 528 nm and 524 nm respectively. We suspect the hypsochromic shift originates from hindered geometric relaxation in the brominated hosts (smaller Stokes shift).

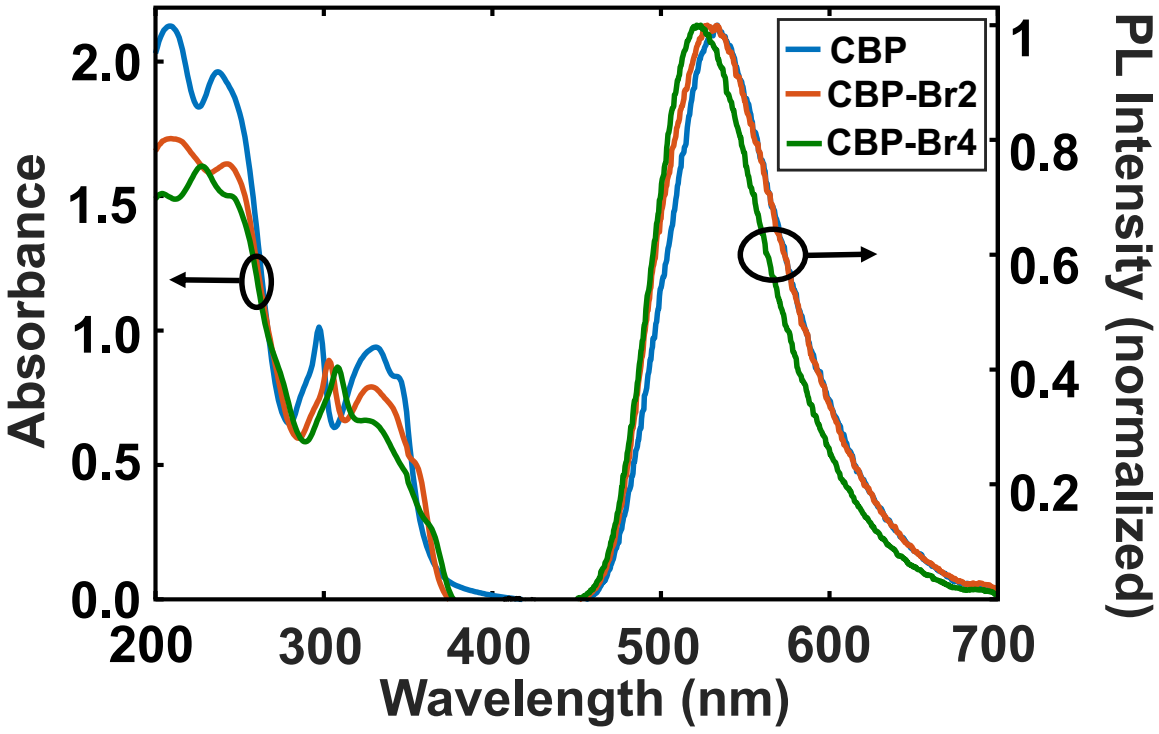

Figure 3. Absorption and emission of EMLs (Host:4CzIPN(20wt%)).

In contrast, the transient photoluminescent response is clearly influenced by the host selection. Firstly, the prompt lifetime for 4CzIPN embedded in CBP is larger than for the brominated compounds (Figure 4a). The prompt lifetimes (τ_p) are 16.7 ns for 4CzIPN in CBP, 10.8 ns for 4CzIPN in CBP-Br2 and 10.9 ns for 4CzIPN in CBP-Br4, indicating that the radiative transition is quenched by an enhanced intersystem crossing rate in the brominated compounds (Table 1). Secondly, the delayed component lifetimes (τ_d) decrease with increasing Br content (Figure 4b). The lifetimes are determined to be 3.49 µs for 4CzIPN in CBP, 3.11 µs for 4CzIPN in CBP-Br2 and 2.92 µs for 4CzIPN in CBP-Br4 respectively. This behavior can be attributed to faster reverse intersystem crossing rate. Thirdly, the delayed components of the brominated CBP derivatives exhibit a larger intensity than CBP. In agreement with aforementioned observations, the ratio of the intensity of the delayed component to the prompt component is growing with increasing Br content (76%, 91% and 92% respectively). The emission spectra of the delayed component (t > 20ns) and prompt components (t < 20ns) are identical for CBP-Br2 (Figure S4) and CBP-Br4 (Figure S5) confirming that $S_0 \leftarrow S_1$ is the dominating radiative transition.

Doped film	Abs. (nm)	PL (nm)	Φ_{PL}	Φ_p	Φ_d	rel. delayed	τ_P (ns)	τ_D (µs)
CBP:4CzIPN	209, 297, 331	534	68%	16%	52%	76%	16.7	3.49
CBP-Br2:4CzIPN	209, 303, 328	528	64%	6%	58%	91%	10.8	3.11
CBP-Br4:4CzIPN	228, 308, 325	524	74%	6%	68%	92%	10.9	2.92

Table 1. Summary of photoluminescent properties for EMLs (Host:4CzIPN(20wt%)).

The photoluminescence quantum yields of the thin films have been determined in an integrating sphere according to the de Mello method.[45] The PLQY for 4CzIPN in CBP was determined to be 68 ± 2%, while the PLQY for the same system with host CBP-Br2 was slightly lower at 64 ± 1%, and higher with the host CBP-Br4 at 74 ± 2%. The prompt and

delayed quantum yields (Φ_p, Φ_d) were calculated from the product of the relative intensities and the absolute PLQY Φ_{PL}. The intersystem crossing rate k_{ISC} and reverse intersystem crossing rate k_{RISC} can then be expressed as:[46,47]

$$k_{ISC} = \frac{\Phi_d}{\Phi_{PL}\tau_p} \quad (1)$$

$$k_{RISC} = \frac{\Phi_d}{\tau_d \tau_p k_{ISC} \Phi_p} \quad (2)$$

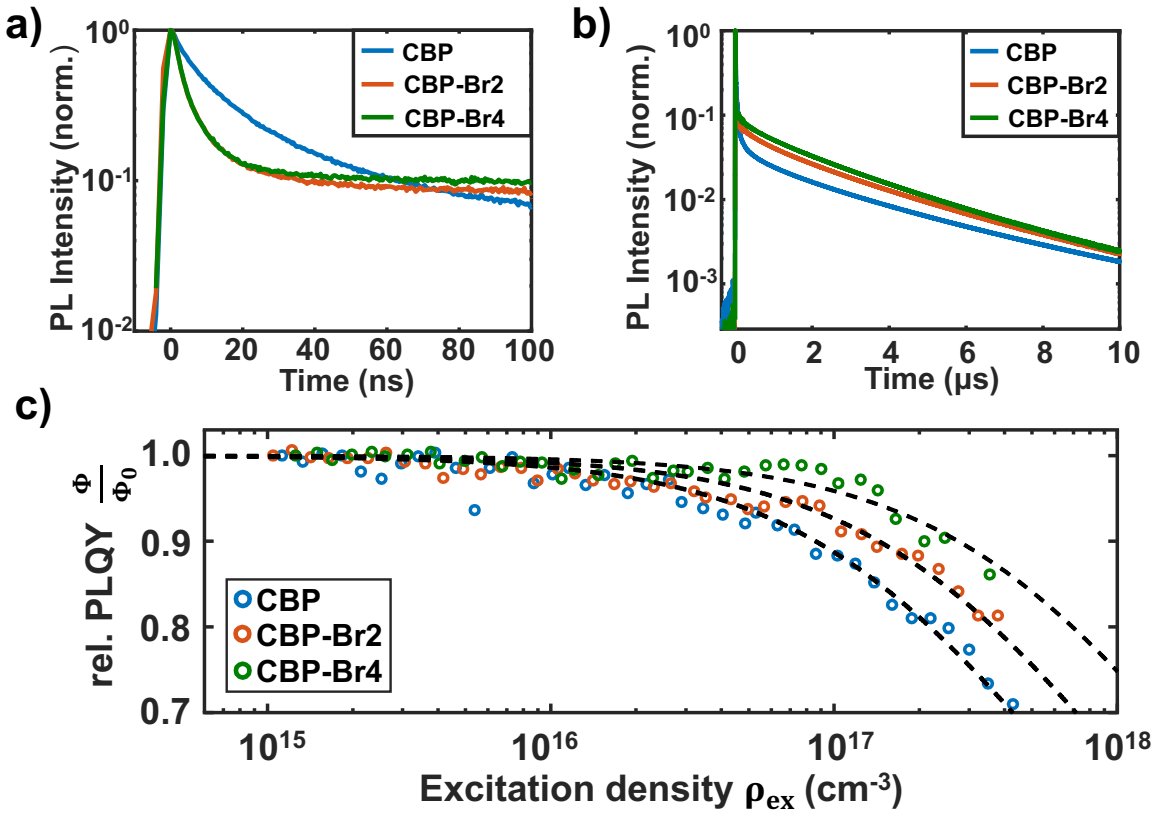

Figure 4. Transient response and PLQY data of EMLs (Host:4CzIPN(20wt%)). **(a)** Prompt component. **(b)** Delayed component. **(c)** Intensity dependence of the PLQY.

The intersystem crossing rates k_{ISC} increased from $4.5 \cdot 10^7\ s^{-1}$ to $8.4 \cdot 10^7\ s^{-1}$ when comparing CBP to its brominated derivatives, which constitutes an 87% increase. The reverse intersystem crossing rates k_{RISC} increased from $1.2 \cdot 10^6\ s^{-1}$ to $3.6 \cdot 10^6\ s^{-1}$and $4.3 \cdot 10^6\ s^{-1}$, which is a 3.0-fold and 3.6-fold increase respectively. The experimental result that k_{RISC} is enhanced to a larger degree than k_{ISC} is in agreement with spectroscopic

ellipsometry measurements of the dielectric constants, which increase with growing number of Br substituents (Figure S15, Table S4). As has been confirmed by a theoretical study recently, singlet-triplet gaps in TADF molecules decrease with increasing dielectric constant.[48] Consequently, the activation energy of the energetically uphill process is reduced and k_{RISC}.is affected both by increased SOC and a lower energy barrier. From the steady state solution of the rate equations we can derive the steady state triplet exciton concentration $[T_1]_{st}$ with respect to the steady state singlet exciton concentration $[S_1]_{st}$ (supporting information).

$$[T_1]_{st} = \frac{k_{ISC}}{k_{RISC}}[S_1]_{st} \quad (3)$$

Therefore, the triplet exciton concentration is 38 times higher than the singlet exciton concentration in the CBP:4CzIPN EML at steady state. This number decreases to 24 (CBP-Br2) and 20 (CBP-Br4) for the brominated compounds. Hence, at constant luminance, the triplet population decreases by 38% and 48% when CBP is replaced by CBP-Br2 and CBP-Br4 respectively (Table 2).

Doped film	k_{ISC} (10^7 s^{-1})	k_{RISC} (10^6 s^{-1})	Rel. [T_1] Steady state	$\rho_{50\%}$ (10^{18})	EQE_{max}	j_{crit} (mA/cm^2)
CBP:4CzIPN	4.6	1.2	100%	1.4	17.1%	22.3
CBP-Br2:4CzIPN	8.4	3.6	62%	2.3	17.9%	24.9
CBP-Br4:4CzIPN	8.4	4.3	52%	4.5	12.4%	>66.7

Table 2. Summary of calculated rate constants, calculated steady state triplet population, $\rho_{50\%}$ values and device characteristics for the EMLs (Host:4CzIPN(20wt%)).

The lower triplet concentrations in these films should have a beneficial influence on bimolecular processes. In order to confirm this, intensity dependent PLQY measurements are conducted on 4CzIPN-doped films made from the different host materials (Figure 4c). All three films exhibit a constant PLQY value for low excitation densities, but start to show a

roll-off for higher excitation densities. We explain this behavior by bimolecular quenching. The onset of the roll-off differs between the different host materials. Brominated CBP hosts are able to sustain high PLQY values for higher excitation densities than their non-brominated counterparts due to their lower triplet exciton concentrations in steady state. The intensity dependence of normalized PLQY can be expressed as:[17]

$$\frac{\Phi_{PL}}{\Phi_0} = \frac{\rho_{50\%}}{4\rho_{ex}}\left(\sqrt{1+\frac{8\rho_{ex}}{\rho_{50\%}}}-1\right) \quad (4)$$

where Φ_{PL} is the PLQY, Φ_0 is the PLQY in the constant regime, ρ_{ex} is the excitation density and $\rho_{50\%}$ is the excitation density at which Φ_{PL} has dropped to 50% of its initial value. The extrapolated values for $\rho_{50\%}$ are $1.4 \cdot 10^{18}$ for CBP to $2.3 \cdot 10^{18}$ and $4.5 \cdot 10^{18}$ for CBP-Br2 and CBP-Br4 respectively. The values of $\rho_{50\%}$ correlate inversely proportional with the square of the steady state triplet concentration, as is expected for a bimolecular process (Figure S7).

The performance of the host materials CBP-Br2 and CBP-Br4 was tested in OLEDs (Figure 5). The optimized device structure is glass / ITO (100nm) / MoO_3 (5 nm) / mCP (50 nm) / Host:4CzIPN(10wt%) (30 nm) / TmPyPb (40 nm) / lithium fluoride (0.7 nm) / Al (100 nm). It was compared to a separately optimized OLED based on the host CBP with the device structure glass / ITO (100nm) / TAPC (40 nm) / mCP (10 nm) / CBP:4CzIPN(10wt%) (30 nm) / TmPyPb (40 nm) / lithium fluoride (0.7 nm) / Al (100 nm). The electroluminescent (EL) spectrum peak of the OLED with the host CBP-Br2 is found at 548 nm (CBP: 553 nm). The maximum EQE of the CBP-Br2 based OLED is determined to be 17.9% (CBP: 17.4%). The critical current density for CBP-Br2 is found at 24.9 mA cm^{-2} (CBP: 22.3 mA cm^{-2}). The device based on CBP-Br2 is on par with the device based on CBP. It shows a slightly higher EQE and lower roll-off. The maximum of the EL spectrum of the device based on CBP-Br4 is found at 545 nm and its maximum EQE is 12.4%. Its maximum EQE value is significantly

lower than the maximum EQE values for the devices based on CBP and CBP-Br2. We attribute this to a charge balance factor significantly below unity. As DFT calculations have shown, the energy levels (HOMO, LUMO) become deeper with increasing number of bromine substitutions (Table S2). As a result, hole injection into the host becomes more difficult. The critical current density for the device based on CBP-Br4 is larger than 66.7 mA cm^{-2}. For current densities higher than 22.6 mA cm^{-2} and at luminances larger than $6.0 \cdot 10^3$ cd m^{-2} it outperforms the device based on CBP in terms of EQE. During our measurements, there were no signs of rapid OLED degradation that would compromise our roll-off analysis. The improved roll-off behavior of the devices based on the brominated hosts is in agreement with the predicted alleviation of bimolecular loss processes like TTA, TCA and singlet-triplet annihilation as a consequence of the lower steady state triplet concentrations. A recent study has also demonstrated better roll-off behavior resulting from increased reverse intersystem crossing rates.[49] However, the roll-off is also influenced by other factors like current dependent charge imbalances and field induced quenching.[20] Therefore it cannot be ascribed to one single cause.

These results also contribute to the clarification of the detailed mechanism of TADF. The proposed mediated process is in agreement with our observations. Varying degrees of spin-orbit coupling influence intersystem crossing between a higher lying triplet exciton T_n (e.g local exciton state ^{3}LE) and the singlet state (e.g. charge transfer state ^{1}CT). Since we observe an increase in intersystem crossing rate in response to the incorporation of heavy atoms into the system, we conclude that the mediated process should be at play. This does not exclude the possibility of additional hyperfine coupling also being present. However, hyperfine coupling is at least an order of magnitude smaller than spin-orbit coupling, unless the latter is suppressed by some selection rule (Figure 1b). If hyperfine coupling was dominant, we

would not have observed a pronounced heavy atom effect as bromine and hydrogen have comparable nuclear magnetic moments. These findings are in accordance with a recently published study that investigates the temperature dependence of the time-resolved photoluminescence of 4CzIPN, wherein the authors confirm the presence of a higher lying triplet state T_n which is involved in the decay process.[50]

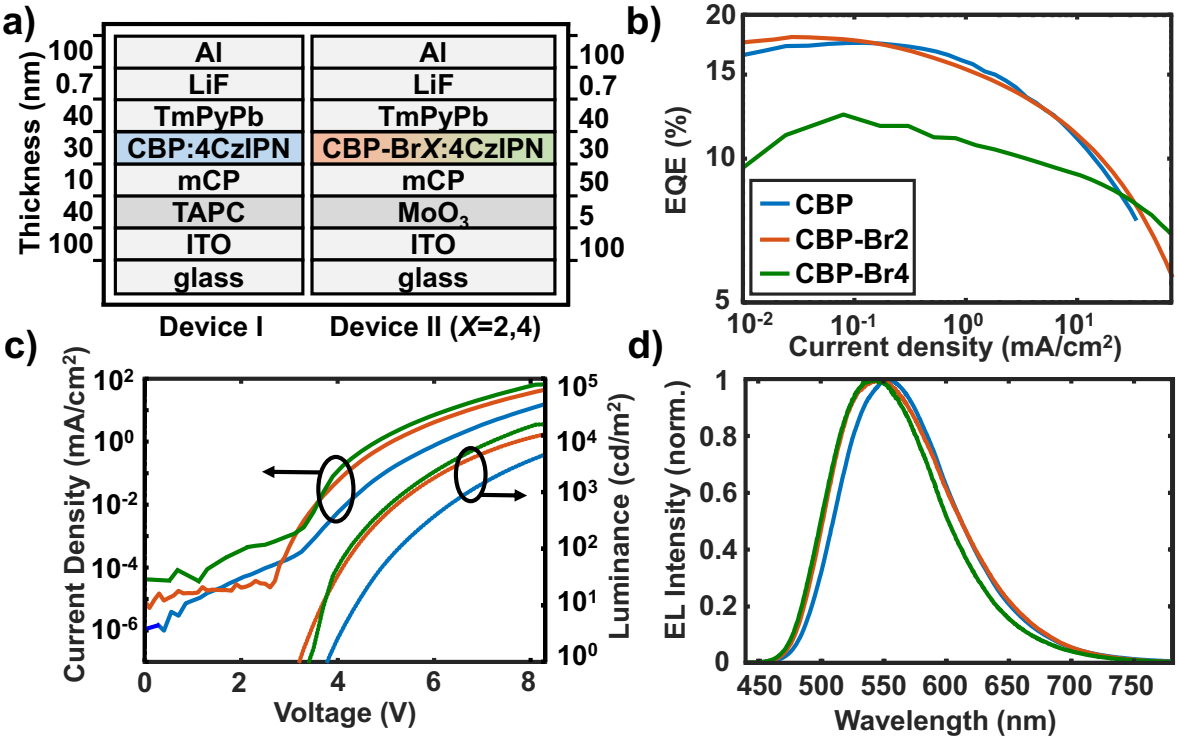

Figure 5. Device data employing brominated hosts CBP-Br2 and CBP-Br4 (Device II) compared to a control device based on CBP (Device I). **(a)** Device structure for devices based on brominated hosts and energy diagram. **(b)** External quantum efficiency vs. current density. **(c)** Current density and luminance vs. applied voltage. **(d)** Electroluminescent spectra.

In conclusion, we have shown that it is possible to reduce exciton lifetimes *via* the external heavy atom effect in a host-guest system without significantly reducing the PLQY or EQE. Our MD and DFT calculations clearly show that the states of host and guest molecules are quantum mechanically coupled in emissive layers. The increase in intersystem crossing rates is due to enhanced spin-orbit coupling. The shorter lifetimes lead to lower triplet exciton densities in the emissive layer in steady state, consequently lowering the frequency of

detrimental bimolecular events. This is evidenced by an improved onset of PLQY droop under high excitation densities. The charge transport properties of the novel heavy atom hosts are sufficient to fabricate highly efficient devices with improved roll-off behavior. These results provide a novel way to alleviate roll-off and potentially degradation in high performance OLEDs by exploiting the external heavy atom effect.

Experimental Section

MD and DFT Calculations: MD with classical OPLS force field is first used to simulate the emission layer structure.[51] The simulations are done using GROMACS computational package (supporting information).[52] 10 random nearest 4CzIPN/CBP dimer structures are extracted from an MD snapshot as the starting structures for DFT calculations. To generate the starting structures of CBP-Br2 and CBP-Br4, we manually replace H atoms in CBP with Br atoms. We then performed ground-state geometry optimizations of these dimer structures using PBE0 functional and 6-31G* basis set.[53] After that, S_0 and T_1 states of all dimers are computed using unrestricted DFT with a larger basis 6-311G**. Subsequently, the Löwdin population analysis of these states is carried out. Electronic structure calculations are done using the Q-Chem package.[54]

Materials: All organic materials are ordered from Luminescence Technology Corp., Taiwan and used as received. Molybdenum trioxide and lithium fluoride were ordered from Sigma Aldrich and used as received. The materials employed in the emissive layer of the OLEDs and doped thin film samples are 4,4'-di(9*H*-carbazol-9-yl)-1,1'-biphenyl (CBP), 4,4'-bis(3-bromo-9*H*-carbazol-9-yl)-1,1'-biphenyl (CBP-Br2) and 4,4'-bis(3,6-dibromo-9*H*-carbazol-9-yl)-1,1'-biphenyl (CBP-Br4) as host materials as well as 2,4,5,6-tetra(9*H*-carbazol-9-yl)isophthalonitrile (4CzIPN) as guest (emitter). In OLEDs Molybdenum trioxide (MoO_3) is employed as hole injection layer (HIL), 4,4-Cyclohexylidenebis[*N,N*-bis(4-

methylphenyl)benzenamine] (TAPC) and 1,3-di(9*H*-carbazol-9-yl)benzene (mCP) as hole transport layers (HTL), 1,3,5-Tris(3-pyridyl-3-phenyl)benzene (TmPyPb) as electron transport layer (ETL) and lithium fluoride (LiF) as electron injection layer (EIL).

Fabrication: Quartz substrates are received from Quartz Scientific, Inc. Pre-patterned indium tin oxide (100nm) glass substrates are received from Luminescence Technology Corp., Taiwan. All substrates are cleaned by sonicating in diluted detergent (Micro-90 cleaning solution), deionized water, acetone and by boiling them in isopropyl alcohol. In case of the OLED substrates, they are subsequently treated with oxygen plasma for 15 minutes. The substrates are transferred to a thermal evaporator directly connected to a nitrogen-filled glovebox. The materials are evaporated through a shadow mask at a base pressure of 10^{-7} Torr and a rate of ~1 Ås^{-1}. Aluminum is evaporated through a contact-defining shadow mask at a base pressure of 10^{-7} Torr and a rate of ~4 Ås^{-1}. The samples are encapsulated using epoxy and cover glass or quartz slides in nitrogen atmosphere with oxygen and moisture levels below 1 ppm.

Measurements: Absorption spectra are taken from doped films (20wt%) of 100 nm thickness in a UV-Vis-NIR Spectrophotometer (Cary 5000, Agilent). Emission spectra are measured with a spectrometer (SP2300, Princeton Instruments) with a 340 nm emitting LED as excitation source (LED, M340L4, Thorlabs). Photoluminescence quantum yields are measured in an integrating sphere (Labsphere) coupled to the aforementioned spectrometer and excited by the same LED. Time resolved photoluminescence measurements are carried out using a picosecond fluorescence lifetime system (Laser Diode 371nm, Streakscope S-20, Hamamatsu, supporting information) or using a photodetector (PDA10A, Thorlabs) connected to an oscilloscope (TDS3054C, Tektronix). Intensity dependent measurements are conducted with a focused laser diode (CPS405, Thorlabs) as excitation source (supporting information). Voltage, current and electroluminescence data are obtained using a precision

semiconductor parameter analyzer (4156C, Agilent) and a silicon photodetector (FDS1010 Thorlabs). During these measurements, the OLED is placed directly on top of a large area photodetector without any intervening optics, so that no correction for wide angle light is required.

Supporting Information
Supporting Information is available from the Wiley Online Library or from the author.

Acknowledgements
This work was supported by the US Department of Energy, Office of Basic Energy Sciences (Award No. DE-FG02-07ER46474).

Received: ((will be filled in by the editorial staff))
Revised: ((will be filled in by the editorial staff))
Published online: ((will be filled in by the editorial staff))

References

[1] M. Segal, M. A. Baldo, R. J. Holmes, S. R. Forrest, Z. G. Soos, *Phys. Rev. B* **2003**, *68*, 75211.
[2] M. A. Baldo, D. F. O'Brien, Y. You, A. Shoustikov, S. Sibley, M. E. Thompson, S. R. Forrest, *Nature* **1998**, *395*, 151.
[3] M. A. Baldo, M. E. Thompson, S. R. Forrest, *Nature* **2000**, *403*, 750.
[4] H. Yersin, A. F. Rausch, R. Czerwieniec, T. Hofbeck, T. Fischer, *Coord. Chem. Rev.* **2011**, *255*, 2622.
[5] M. A. Baldo, S. Lamansky, P. E. Burrows, M. E. Thompson, S. R. Forrest, *Appl. Phys. Lett.* **1999**, *75*, 4.
[6] C. Adachi, M. A. Baldo, M. E. Thompson, S. R. Forrest, *J. Appl. Phys.* **2001**, *90*, 5048.
[7] H. Uoyama, K. Goushi, K. Shizu, H. Nomura, C. Adachi, *Nature* **2012**, *492*, 234.
[8] H. Tanaka, K. Shizu, H. Miyazaki, C. Adachi, *Chem. Commun.* **2012**, *48*, 11392.
[9] J. Lee, K. Shizu, H. Tanaka, H. Nomura, T. Yasuda, C. Adachi, *J. Mater. Chem. C* **2013**, *1*, 4599.
[10] F. B. Dias, J. Santos, D. R. Graves, P. Data, R. S. Nobuyasu, M. A. Fox, A. S. Batsanov, T. Palmeira, M. N. Berberan-Santos, M. R. Bryce, A. P. Monkman, *Adv. Sci.* **2016**, *3*, 1600080.
[11] E. Hontz, W. Chang, D. N. Congreve, V. Bulović, M. A. Baldo, T. Van Voorhis, *J. Phys. Chem. C* **2015**, *119*, 25591.
[12] Y. Sheng, T. D. Nguyen, G. Veeraraghavan, Ö. Mermer, M. Wohlgenannt, S. Qiu, U. Scherf, *Phys. Rev. B* **2006**, *74*, 45213.
[13] H. Malissa, M. Kavand, D. P. Waters, K. J. van Schooten, P. L. Burn, Z. V. Vardeny, B. Saam, J. M. Lupton, C. Boehme, *Science* **2014**, *345*, 1487.
[14] M. K. Etherington, J. Gibson, H. F. Higginbotham, T. J. Penfold, A. P. Monkman, *Nat. Commun.* **2016**, *7*, 13680.
[15] R. S. Nobuyasu, Z. Ren, G. C. Griffiths, A. S. Batsanov, P. Data, S. Yan, A. P. Monkman, M. R. Bryce, F. B. Dias, *Adv. Opt. Mater.* **2016**, *4*, 597.

[16] M. Pope, C. E. Swenberg, *Electronic Processes in Organic Crystals and Polymers*, Oxford University Press, **1999**.
[17] M. A. Baldo, C. Adachi, S. R. Forrest, *Phys. Rev. B* **2000**, *62*, 10967.
[18] C. E. Swenberg, N. Geacintov, J. B. Birks, *Organic Molecular Photophysics*, John Wiley, New York, **1973**.
[19] D. Hertel, K. Meerholz, *J. Phys. Chem. B* **2007**, *111*, 12075.
[20] C. Murawski, K. Leo, M. C. Gather, *Adv. Mater.* **2013**, *25*, 6801.
[21] S. Schmidbauer, A. Hohenleutner, B. König, *Adv. Mater.* **2013**, *25*, 2114.
[22] H. Cang, Y. Liu, Y. Wang, X. Yin, X. Zhang, *Nano Lett.* **2013**, *13*, 5949.
[23] R. Gómez-Bombarelli, J. Aguilera-Iparraguirre, T. D. Hirzel, D. Duvenaud, D. Maclaurin, M. A. Blood-Forsythe, H. S. Chae, M. Einzinger, D.-G. Ha, T. Wu, G. Markopoulos, S. Jeon, H. Kang, H. Miyazaki, M. Numata, S. Kim, W. Huang, S. I. Hong, M. Baldo, R. P. Adams, A. Aspuru-Guzik, *Nat. Mater.* **2016**, *15*, 1120.
[24] A. Kretzschmar, C. Patze, S. T. Schwaebel, U. H. F. Bunz, *J. Org. Chem.* **2015**, *80*, 9126.
[25] M. Kasha, *J. Chem. Phys.* **1952**, *20*, 71.
[26] S. P. McGlynn, M. J. Reynolds, G. W. Daigre, N. D. Christodoyleas, *J. Phys. Chem.* **1962**, *66*, 2499.
[27] M. Rae, A. Fedorov, M. N. Berberan-Santos, *J. Chem. Phys.* **2003**, *119*, 2223.
[28] M. Rae, F. Perez-Balderas, C. Baleizão, A. Fedorov, J. A. S. Cavaleiro, A. C. Tomé, M. N. Berberan-Santos, *J. Phys. Chem. B* **2006**, *110*, 12809.
[29] C. Baleizão, M. N. Berberan-Santos, *ChemPhysChem* **2010**, *11*, 3133.
[30] P. Xue, P. Wang, P. Chen, B. Yao, P. Gong, J. Sun, Z. Zhang, R. Lu, *Chem. Sci.* **2016**, DOI 10.1039/C5SC03739E.
[31] X. Sun, B. Zhang, X. Li, C. O. Trindle, G. Zhang, *J. Phys. Chem. A* **2016**, *120*, 5791.
[32] D. Zhang, L. Duan, Y. Zhang, M. Cai, D. Zhang, Y. Qiu, *Light Sci. Appl.* **2015**, *4*, e232.
[33] W. Zhang, J. Jin, Z. Huang, S. Zhuang, L. Wang, *Sci. Rep.* **2016**, *6*, DOI 10.1038/srep30178.
[34] S. Suzuki, *Charge Carrier Material, Organic Electroluminescent Element, and Indicator Panel*, **2005**, JP 2005071909.
[35] P. Stoessel, E. Breuning, A. Buesing, A. Parham, H. Heil, H. Vestweber, *Organic Electronic Devices and Boronic Acid and Boronic Acid Derivatives Used Therein*, **2006**, WO2006117052.
[36] S. Funyu, K. Ishitsuka, Y. Hoshi, *Organic Electronic Material, Ink Composition Containing Same, and Organic Thin Film, Organic Electronic Element, Organic Electroluminescent Element, Lighting Device, and Display Device Formed Therewith*, **2010**, WO2010140553.
[37] K. Ishizuka, Y. Hoshi, S. Funyu, Y. Morishita, *Organic Materials for Organic Electronics*, **2009**, JP2009267393.
[38] M. D. Andrews, K. Look, A. Mosley, A. R. Steudel, N. Male, N. Maxted, *Phosphorescent Compositions and Organic Light Emitting Devices Containing Them*, **2003**, WO2003074628.
[39] U. Stoeck, S. Krause, V. Bon, I. Senkovska, S. Kaskel, *Chem. Commun.* **2012**, *48*, 10841.
[40] M. R. Talipov, M. M. Hossain, A. Boddeda, K. Thakur, R. Rathore, *Org. Biomol. Chem.* **2016**, *14*, 2961.
[41] İ. Kaya, K. Temizkan, A. Aydın, *Mater. Sci. Eng. B* **2013**, *178*, 863.
[42] S. Reineke, M. A. Baldo, *Sci. Rep.* **2014**, *4*, DOI 10.1038/srep03797.
[43] K. Goushi, R. Kwong, J. J. Brown, H. Sasabe, C. Adachi, *J. Appl. Phys.* **2004**, *95*, 7798.
[44] P.-O. Löwdin, *J. Chem. Phys.* **1950**, *18*, 365.

[45] J. C. de Mello, H. F. Wittmann, R. H. Friend, *Adv. Mater.* **1997**, *9*, 230.
[46] K. Goushi, K. Yoshida, K. Sato, C. Adachi, *Nat. Photonics* **2012**, *6*, 253.
[47] Y. Tao, K. Yuan, T. Chen, P. Xu, H. Li, R. Chen, C. Zheng, L. Zhang, W. Huang, *Adv. Mater.* **2014**, *26*, 7931.
[48] H. Sun, Z. Hu, C. Zhong, X. Chen, Z. Sun, J.-L. Brédas, *J. Phys. Chem. Lett.* **2017**, *8*, 2393.
[49] C.-K. Moon, K. Suzuki, K. Shizu, C. Adachi, H. Kaji, J.-J. Kim, *Adv. Mater.* **2017**, DOI 10.1002/adma.201606448.
[50] T. Kobayashi, A. Niwa, K. Takaki, S. Haseyama, T. Nagase, K. Goushi, C. Adachi, H. Naito, *Phys. Rev. Appl.* **2017**, *7*, 34002.
[51] W. L. Jorgensen, D. S. Maxwell, J. Tirado-Rives, *J. Am. Chem. Soc.* **1996**, *118*, 11225.
[52] B. Hess, C. Kutzner, D. Van Der Spoel, E. Lindahl, *J. Chem. Theory Comput.* **2008**, *4*, 435.
[53] C. Adamo, V. Barone, *J. Chem. Phys.* **1999**, *110*, 6158.
[54] Y. Shao, Z. Gan, E. Epifanovsky, A. T. B. Gilbert, M. Wormit, J. Kussmann, A. W. Lange, A. Behn, J. Deng, X. Feng, D. Ghosh, M. Goldey, P. R. Horn, L. D. Jacobson, I. Kaliman, R. Z. Khaliullin, T. Kuś, A. Landau, J. Liu, E. I. Proynov, Y. M. Rhee, R. M. Richard, M. A. Rohrdanz, R. P. Steele, E. J. Sundstrom, H. L. W. III, P. M. Zimmerman, D. Zuev, B. Albrecht, E. Alguire, B. Austin, G. J. O. Beran, Y. A. Bernard, E. Berquist, K. Brandhorst, K. B. Bravaya, S. T. Brown, D. Casanova, C.-M. Chang, Y. Chen, S. H. Chien, K. D. Closser, D. L. Crittenden, M. Diedenhofen, R. A. D. Jr, H. Do, A. D. Dutoi, R. G. Edgar, S. Fatehi, L. Fusti-Molnar, A. Ghysels, A. Golubeva-Zadorozhnaya, J. Gomes, M. W. D. Hanson-Heine, P. H. P. Harbach, A. W. Hauser, E. G. Hohenstein, Z. C. Holden, T.-C. Jagau, H. Ji, B. Kaduk, K. Khistyaev, J. Kim, J. Kim, R. A. King, P. Klunzinger, D. Kosenkov, T. Kowalczyk, C. M. Krauter, K. U. Lao, A. D. Laurent, K. V. Lawler, S. V. Levchenko, C. Y. Lin, F. Liu, E. Livshits, R. C. Lochan, A. Luenser, P. Manohar, S. F. Manzer, S.-P. Mao, N. Mardirossian, A. V. Marenich, S. A. Maurer, N. J. Mayhall, E. Neuscamman, C. M. Oana, R. Olivares-Amaya, D. P. O'Neill, J. A. Parkhill, T. M. Perrine, R. Peverati, A. Prociuk, D. R. Rehn, E. Rosta, N. J. Russ, S. M. Sharada, S. Sharma, D. W. Small, A. Sodt, T. Stein, D. Stück, Y.-C. Su, A. J. W. Thom, T. Tsuchimochi, V. Vanovschi, L. Vogt, O. Vydrov, T. Wang, M. A. Watson, J. Wenzel, A. White, C. F. Williams, J. Yang, S. Yeganeh, S. R. Yost, Z.-Q. You, I. Y. Zhang, X. Zhang, Y. Zhao, B. R. Brooks, G. K. L. Chan, D. M. Chipman, C. J. Cramer, W. A. G. III, M. S. Gordon, W. J. Hehre, A. Klamt, H. F. S. III, M. W. Schmidt, C. D. Sherrill, D. G. Truhlar, A. Warshel, X. Xu, A. Aspuru-Guzik, R. Baer, A. T. Bell, N. A. Besley, J.-D. Chai, A. Dreuw, B. D. Dunietz, T. R. Furlani, S. R. Gwaltney, C.-P. Hsu, Y. Jung, J. Kong, D. S. Lambrecht, W. Liang, C. Ochsenfeld, V. A. Rassolov, L. V. Slipchenko, J. E. Subotnik, T. V. Voorhis, J. M. Herbert, Anna I., *Mol. Phys.* **2015**, *113*, 184.